NASA Technical Memorandum 84363

Trends of Reynolds Number Effects on Two-Dimensional Airfoil Characteristics for Helicopter Rotor Analyses

G. K. Yamauchi and Wayne Johnson

April 1983

National Aeronautics and
Space Administration

NASA Technical Memorandum 84363

Trends of Reynolds Number Effects on Two-Dimensional Airfoil Characteristics for Helicopter Rotor Analyses

G. K. Yamauchi,
Wayne Johnson, Ames Research Center, Moffett Field, California

National Aeronautics and
Space Administration

Ames Research Center
Moffett Field, California 94035

TRENDS OF REYNOLDS NUMBER EFFECTS ON TWO-DIMENSIONAL AIRFOIL CHARACTERISTICS FOR HELICOPTER ROTOR ANALYSES

G. K. Yamauchi

and

Wayne Johnson

Summary

The primary effects of Reynolds number on two-dimensional airfoil characteristics are discussed. Results from an extensive literature search reveal the manner in which the minimum drag and maximum lift are affected by the Reynolds number. $C_{d_{min}}$ and $C_{\ell_{max}}$ are plotted versus Reynolds number for airfoils of various thickness and camber. From the trends observed in the airfoil data, universal scaling laws and easily implemented methods are developed to account for Reynolds number effects in helicopter rotor analyses.

NOMENCLATURE

a	speed of sound
c	airfoil chord
c_d	two-dimensional drag coefficient, drag/$1/2\rho V^2 c$
$c_{d_{min}}$	minimum drag coefficient
c_f	flat plate skin friction coefficient
c_ℓ	two-dimensional lift coefficient, lift/$1/2\rho V^2 c$
$c_{\ell_{max}}$	maximum lift coefficient
c_m	two-dimensional moment coefficient, moment/$1/2\rho V^2 c^2$
K	Reynolds number correction factor
M	Mach number, V/a
R_e	Reynolds number, Vc/ν
V	air velocity
α	angle of attack
α_{max}	angle of attack at maximum lift coefficient
α_{ZL}	angle of attack at zero lift
μ	viscosity
ν	kinematic viscosity, μ/ρ
ρ	air density

Subscript:

t	airfoil table

Abbreviations:

FST	NACA Full-Scale Wind Tunnel (9.144 by 18.288-meter)
VDT	NACA Variable-Density Wind Tunnel (1.524-meter diameter)
LTT	NACA Two-Dimensional Low Turbulence Tunnel (0.9144 by 2.286-meter)
TDT	NACA Two-Dimensional Low Turbulence Pressure Tunnel (0.9144- by 2.286-meter)

INTRODUCTION

Analyses of helicopter rotor behavior are almost universally based on lifting-line theory, in which the inner problem is a two-dimensional airfoil in an aerodynamic environment determined by the rotor wake (see for example, ref. 1). The solution of this inner problem often is based on the use of experimental airfoil data for the lift, drag, and moment coefficients as a function of angle-of-attack and Mach number. Experimental characteristics are used in order to account for real flow effects, including stall and compressibility effects. The data are provided in the form of a table, so interpolation is necessary to evaluate the coefficients at a given angle-of-attack and Mach number. Such airfoil data are obtained from two-dimensional wind tunnel tests.

Viscous effects, as governed by the Reynolds number $Re = Vc/\nu$, have a major influence on the airfoil lift, drag, and moment characteristics. Hence it is important that the airfoil data used for helicopter rotor analyses be for the correct Reynolds number. For a constant chord, the Reynolds number is proportional to the Mach number, and the data in the airfoil tables at each Mach number must be for the corresponding Reynolds number. If the rotor blade chord varies radially, it will be necessary to have data corresponding to the Reynolds number at each radial station where the aerodynamic loads are evaluated in the analyses.

If experimental airfoil data at the proper Reynolds number for the analysis of a particular rotor are not available, it will be necessary to apply corrections to whatever data are available. The current practice in the helicopter industry is generally as follows. Often special airfoil tests

are conducted for a specific helicopter to obtain data at exactly the desired Reynolds number (preferably including the correct effects of roughness and boundary layer transition as well). When it is necessary to correct existing data for Reynolds number effects, particularly the drag and stall characteristics, the corrections are defined using state-of-the-art airfoil design and analysis methods (typically computational fluid dynamics codes). When the chord changes are small, or results are required quickly, simple correction procedures are used, commonly scaling the drag coefficient with the one-fifth power of Reynolds number or defining a single drag coefficient increment based on some scaling law.

Reynolds number effects on rotor airfoil characteristics are also of concern because they determine the influence of scale on rotor behavior. The influence of scale must be considered when designing a helicopter larger or smaller than the size from which the design data base comes. When small-scale tests are conducted in the course of helicopter rotor research and development, Reynolds number effects must be considered in order to properly estimate the rotor behavior at full scale.

The objective of the present paper is to discuss the primary effects of Reynolds number on two-dimensional airfoil characteristics. The results will serve as a guide in identifying the influence of scale on helicopter rotor characteristics and in the development of Reynolds number corrections of airfoil tables for rotor analyses. An extensive search through the literature was performed to catagorize the effects of Reynolds number. The maximum lift coefficient and minimum drag coefficient were found to be greatly affected by

Reynolds number. Consequently, this paper is primarily concerned with those two quantities. Data from the literature are presented to illustrate the effect of Reynolds number on $c_{d_{min}}$ and $c_{\ell_{max}}$ for airfoils of various thickness and camber. The effect of roughness is also examined. The data have been faired to show general trends; the cited references give the exact data points. A Reynolds number range of 10^5 to 10^7 was considered, since this is the regime in which a typical rotor blade operates. The effect of Reynolds number on the drag coefficient was of particular interest, since results could be compared with several formulas for the skin-friction of a flat plate. The paper therefore begins with a discussion of flat plate skin friction drag. The results from the available literature on the variations of airfoil characteristics with Reynolds number are then summarized and discussed. Finally, some simple correction procedures for Reynolds number effects are described.

BACKGROUND ON SKIN FRICTION DRAG

The relationship between the drag coefficient of an airfoil and the Reynolds number can be better understood by first studying a flat plate situated parallel to an oncoming flow. The plate will experience only skin friction drag, as the pressure drag will ideally be zero. For a low Reynolds number, the flow over the plate will be mainly laminar. According to ref. 2, the law of friction for a flat plate in laminar flow was first developed by Blasius, and is given by:

$$c_f = 1.328\ Re^{-0.5} \quad \text{for } Re < 5\times10^5 \text{ or } 10^6 \qquad \text{(Eq. 1)}$$

This law holds for a flat plate at zero incidence in two-dimensional flow.

As the Reynolds number increases, the boundary layer adjacent to the plate undergoes a transition from a laminar to a turbulent boundary layer. Numerous experiments have been performed to predict the flat plate turbulent skin friction drag as a function of Reynolds number. To date there is no exact solution; existing formulas are based largely on experimental data.

From the investigations of turbulent flows in pipes by Blasius in 1911 came the Blasius resistance formula in terms of Reynolds number (ref. 2). With the results of experiments investigating the law of friction and velocity profiles in smooth pipes by Nikuradse, Blasi us's formula can be related to a one-seventh power velocity-distribution law. By assuming the velocity profiles in the boundary layer of a smooth flat plate and a smooth pipe are identical, the following formula by Prandtl results for the skin friction drag coefficient of a smooth flat plate whose boundary layer is turbulent from the leading edge onwards:

$$c_f = 0.074\ Re^{-0.2} \quad \text{for } 5\times10^5 < Re < 10^7 \qquad \text{(Eq. 2)}$$

(ref.2). A formula for c_f was also developed by Prandtl from the logarithmic velocity-distribution law (ref. 2). From Prandtl's analysis, Schlichting developed an empirical relationship between c_f and Reynolds number:

$$c_f = \frac{0.455}{(\log Re)^{2.58}}$$

To account for any initial laminar flow along the plate, a decrement is included in the above equation for c_f:

$$c_f = \frac{0.455}{(\log Re)^{2.58}} - \frac{A}{Re} \quad \text{for } Re \leq 10^9 \qquad \text{(Eq. 3)}$$

where A depends upon the location of the point of transition from a laminar

to a turbulent boundary layer. Equation 3 is the Prandtl-Schlichting skin-friction formula for a smooth flat plate at zero incidence with a turbulent boundary layer (ref.2).

Several other formulas for flat plate skin friction drag with a turbulent boundary layer are also available. According to ref. 3, von Karman determined that c_f is proportional to log(Re c_f). From this relationship, Schoenherr developed the following formula:

$$\log (\mathrm{Re}\ c_f) = 0.242\ c_f^{-0.5} \quad \text{for Re} \leq 10^9 \text{ or } 10^{10} \qquad \text{(Eq. 4)}$$

An approximation to Schoenherr's formula is given in ref. 3 as:

$$c_f^{-0.5} = 3.46 \log \mathrm{Re} - 5.6 \qquad \text{(Eq. 5)}$$

By experimenting with velocity distributions on a plane wall, Schultz-Grunow developed the following formula (ref. 3)

$$c_f = 0.427\ (\log \mathrm{Re} - 0.407)^{-2.64} \quad \text{for Re} \leq 10^9 \qquad \text{(Eq. 6)}$$

Eqs. 4 and 6 agree well with experimental results (according to ref. 3), and are valid over a larger range of Reynolds number than eq. 2. However, eqs. 4 and 6 do not account for the transition region. A decrement such as the one included in eq. 3 should be included in eqs. 4 and 6, if the c_f in the transition region is desired.

Figure 1 shows plots of flat plate skin friction drag for laminar and turbulent flow, including the transition region, based on eqs. 1, 3, and 4. The quantity $2c_f$ is plotted for comparison with airfoil drag coefficient values. The form of these curves is characteristic of the variation of airfoil drag with Reynolds number as well.

SUMMARY OF EXPERIMENTAL RESULTS

A review of the literature on two-dimensional airfoil characteristics established that the lift and drag coefficients are greatly affected by Reynolds number, while there is little or no effect on moment coefficient (or at least no generalizable effect; see for example, ref. 4). The results to be presented here were obtained from refs. 4-18. Correlating the results from the literature was difficult, as no two experiments were performed under the same test conditions. Table 1 indicates some factors that must be considered when comparing results from different sources, including type of wind tunnel used, airfoil chord, airfoil span, and the type of correction applied to the test data. The figures to be discussed reflect the discrepancies between the sources. However, the various sources show similar trends for the characteristics of a given airfoil (with a few exceptions).

Minimum Drag Coefficient

Figure 2 shows the minimum drag coefficient as a function of Reynolds number for the NACA 0012 airfoil. The curve from NACA Rept. 586 (VDT) evidently includes the transition region of the flow, since $c_{d_{min}}$ decreases, increases, and then decreases with Reynolds number (compare with fig. 1). NACA Rept. 669 shows the same test data as Rept. 586, with additional data reduction corrections as specified in Rept. 669. The remaining curves show no sign of a transition region. The slopes of all curves are roughly -0.125 or less for Re greater than approximately 4×10^6. Leading edge roughness

caused $c_{d_{min}}$ to increase by as much as 0.0065, according to NACA TN 1945. However, the increment in drag due to roughness decreases as Re increases. One-hundred per-cent turbulent flow (i.e. with the transition point at the leading edge) caused the drag to increase by as much 0.0022, according to NACA War Rept. L-682. This increment also decreased with increasing Re. An interpretation of this trend can be that the addition of roughness to an airfoil increases the effect of the Reynolds number (the NACA TN 1945 curves show this). It should be noted that drag values in NACA War Rept. L-682 were obtained computationally, based on experimental determination of the transition point on the airfoil.

Data from NACA Rept. 586 are shown in several of the figures to follow. The corrections described in NACA Rept. 669 can be applied to all of the curves obtained from NACA Rept. 586. An example of the form and magnitude of these corrections on the drag data is shown in fig. 2 (compare the plots from NACA Repts. 586 and 669). Data obtained from NACA Repts. 647 and 530 (shown in figs. 2 and 3, respectively) apply to a rectangular, aspect ratio 6 wing. In NACA Rept. 647 it is shown that the wing minimum drag behaves similarly to the section drag coefficient, requiring only a small correction for tip effects. The plot shown in fig. 2 from NACA Rept. 647 has been corrected for tip effects.

Figure 3 shows the minimum drag coefficient as a function of Reynolds number for the NACA 23012 airfoil. NACA TN 1945 shows $c_{d_{min}}$ is increased by as much as 0.0062 by leading edge roughness, with the drag increment decreasing as Re inceases. Elimination of the drag bucket in the drag versus lift graphs in NACA TN 1945 brings the $c_{d_{min}}$ versus Re curve into better agreement

with the other plots. NACA Rept. 586 again shows a transition region. Curves from NACA Rept. 586, Rept. 530, and TN 1945 (LE roughness) have slopes of approximately -0.125. Although not shown in this figure, NACA Rept. 530 also gives results obtained in the FST, which produced lower values of $c_{d_{min}}$ than the VDT results.

Drag data for two helicopter rotor airfoils are presented in fig. 4. The minimum drag appears to decrease with increasing Re for the SC1095-R8, while the drag first decreases and then increases for the SC1095 airfoil. Since NASA TP 1701 offered $c_{d_{min}}$ values at only a few Reynolds numbers, these trends are not necessarily correct. However, the SC1095 shows lower drag values than the SC1095-R8, which is a modification of the SC1095 including a drooped leading edge.

The effect of thickness on the minimum drag coefficient as a function of Reynolds number is illustrated in figs. 5 and 6, for the NACA 230-series and 63-series airfoils, respectively. For Re less than approximately 8×10^6, both figures show that $c_{d_{min}}$ increases with thickness at a constant Reynolds number. It should be noted that NACA RM L8B02 (fig. 5) gives data for the drag at the design lift coefficient, which is $c_\ell = 0.3$ for the 230-series airfoil. The actual minimum drag occurs at a lower value of lift, around $c_\ell = 0.1$ or 0.2. The curve from NACA War Rept. L-752 (fig. 5) is the drag at a lift coefficient of $c_\ell = 0.275$. Figure 5 shows that the effect of Reynolds number increases with thickness; i.e. the slope of $c_{d_{min}}$ versus Re increases in magnitude as thickness increases. The Reynolds number effect on the 63-series airfoils is shown in fig. 6. Contrary to the 230-series result, fig.

6 shows that for each airfoil the drag increases after a certain Reynolds number has been reached.

Figure 7 shows that at a constant Reynolds number, the minimum drag increases as the point of minimum pressure moves forward on the chord. For these airfoils $c_{d_{min}}$ is insensitive to Re below about 9×10^6, after which the drag increases with a slope of approximatley 0.33. The influence of the thickness form however is a uniform increment in drag, independent of Reynolds number over the range covered by NACA TN 1773.

Maximum Lift Coefficient

The lift curve slope and the angle of zero lift of an airfoil section remain relatively unchanged as the Reynolds number varies (see, for example, ref. 4). Hence this section is only concerned with the Reynolds number influence on the maximum lift.

Figures 8-11 give the maximum lift coefficient as a function of Reynolds number for respectively the NACA 0012, NACA 23012, and several helicopter airfoils. In general, $c_{\ell_{max}}$ increases with Re for curves on all of these figures. Figure 8 shows data for the NACA 0012 section. All curves show $c_{\ell_{max}}$ increasing with Re. According to NACA TN 1945, adding leading edge roughness introduces a decrement of a least 0.2 to the value of $c_{\ell_{max}}$ for a smooth NACA 0012 airfoil. The magnitude of this decrement increases with increasing Re. Hence roughness lessens the effect of Reynolds number on $c_{\ell_{max}}$. Figure 9 presents data for the NACA 23012 airfoil section. It should be noted that NACA TN 1945 used data from ref. 4 for $3 \times 10^6 \leq$ Re $\leq$

$9x10^6$, hence the coincidence of the two curves for this Reynolds number range. The effects of roughness are similar to those on the NACA 0012 section. The curves of fig. 8 show a wide range of slopes. The slopes of the curves of fig. 9 fall in the 0.125 to 0.2 range. The data obtained from NACA Repts. 647 and 530 (shown in figs. 8, 9, and 13) apply to a rectangular, aspect ratio 6 wing. NACA Rept. 647 shows that for the NACA 0012 and 0009 airfoils, the wing stalls simultaneously over the span, suggesting that the maximum lift should be comparable to that of the two-dimensional airfoil.

Figure 10 shows the $c_{\ell_{max}}$ characteristics of five early NACA helicopter airfoils. Because of the limited data obtainable from NACA TN 1922, definite trends are not discernible. Figure 11 shows the $c_{\ell_{max}}$ characteristics of three currently used helicopter airfoils: the SC1095, SC1095-R8, and the NACA 0012 with 0-deg tab. The maximum lift increases with increasing Re for the SC1095-R8 and the NACA 0012 with 0-deg tab, while the SC1095 shows little variation of $c_{\ell_{max}}$ with Reynolds number.

The effect of thickness on $c_{\ell_{max}}$ versus Re curves is shown in figs. 12-14 for various sets of airfoils. For Re less than approximately $1.5x10^6$, NACA Rept. 586 shows in fig. 12 that $c_{\ell_{max}}$ increases with increasing thickness at constant Re, an effect that diminishes as Reynolds number increases. The thinner airfoils (NACA 0012 and 0009 sections) show a delayed response to Reynolds number effects. For Reynolds number above $1.5x10^6$, NACA TN 3524 shows (fig. 13) that the effect of thickness increases with increasing Re. The thinnest section, the NACA 0006, seems to show a slight decrease in $c_{\ell_{max}}$ with increasing Re. Data for the NACA 0009 are shown from two sources. The two curves are significantly different; the curve obtained from NACA Rept.

647 matches well the curves from NACA TN 3524. The slopes of the curves for the NACA 0007, 0008, and 0009 airfoils are approximately 0.125. The NACA 63-series of airfoils show similar trends for $c_{\ell_{max}}$ versus Re (fig. 14). The Reynolds number effects is again greatest for the thickest airfoil.

Figure 15 shows the influence of camber on the variation of $c_{\ell_{max}}$ with Reynolds number. The maximum lift increases with camber for a constant Re. Similar effects are found for the NACA 63-series airfoil data in NACA TN 1773 (not shown here). As camber increases, the effect of Reynolds number decreases. Also, the influence of camber decreases as Re increases.

The effect of thickness form (the chordwise position of the point of minimum pressure) on the $c_{\ell_{max}}$ characteristics is shown in fig. 16. The maximum lift coefficient for all three airfoils remains relatively unaffected over the range $3\times10^6 < Re < 9\times10^6$. For Reynolds number greater than approximately 1.2×10^7, $c_{\ell_{max}}$ increases with increasing Re. With constant Reynolds number, $c_{\ell_{max}}$ increases with decreasing thickness form for $Re > 1.2\times10^7$.

Compressibility Effects

The effect of Mach number must also be considered in analyzing the influence of Reynolds number. The data presented in figs. 2-16 are generally for low Mach number (see table 1). There is evidence that there is a particular Mach number above which the effect of Reynolds number on $c_{\ell_{max}}$ is insignificant and the effect of compressibility dominates. For the NACA 0012 rectangular wing, as tested in ref. 19, compressibility had a major effect on the values of $c_{\ell_{max}}$ for Mach numbers above about 0.17, while the Reynolds number effect dominated for Mach numbers below 0.17. Ref. 20 reports that

Mach number as well as Reynolds number effects must be considered when correlating data from different wind tunnels (and flight tests). Reference 20 shows that the Reynolds number effect decreased progressively as Mach number increased, becoming insignificant at a Mach number of approximately 0.55. Reference 21 shows $c_{\ell_{max}}$ versus Re for three different variations of Mach number with Reynolds number; the conclusion was made that for Mach numbers above 0.15-0.20, compressibility effects become serious. Reference 14 shows that for rough airfoils, the Reynolds number effect on $c_{\ell_{max}}$ was nearly the same, regardless of how Mach number varied with Reynolds number; ref. 22 shows similar trends. Although $c_{\ell_{max}}$ increases with increasing Reynolds number, it decreases with increasing Mach number. Reference 23 states that $c_{\ell_{max}}$ is almost entirely dependent on Reynolds number below a particular Mach number, yet Mach number effects should not be neglected for even low Mach numbers.

SIMPLE CORRECTIONS FOR REYNOLDS NUMBER EFFECTS

It is useful to have universally applicable and easily implemented methods to correct airfoil data for the influence of Reynolds number. The airfoil data are normally available for helicopter rotor analyses in tabular form: values of lift, drag, and moment coefficient at discrete values of angle-of-attack and Mach number. Linear interpolation is used to evaluate the coefficients at arbitrary angle-of-attack and Mach number. Equations are required to then correct the coefficients from the Reynolds number of the table to the actual Reynolds number of the rotor blade section.

The description of the airfoil table must now include a list of Reynolds number values, one for each Mach number value in the table. For an arbitrary Mach number, the Reynolds number list can be linearly interpolated to find the corresponding Reynolds number value.

The Reynolds number can be written $Re = (V/a)\ (ca/\nu) = M\ Re_1$, where a is the speed of sound. For the airfoil table, Re_1 will be a constant if the airfoil was tested at constant pressure and temperature (which is possible, but not always done). For the rotor blade, Re_1 will be a constant if the chord is constant. If both conditions are satisfied, then it follows that $Re_t/Re = Re_{1t}/Re_1$ = constant, regardless of the Mach number (here the subscript "t" refers to the table values).

The airfoil characteristics presented in the preceeding sections provide justification for the assumption that universal scaling equations may be applied to account for the influence of Reynolds number. These experimental results also provide guidance for selecting the specific forms of the scaling equations, and for assessing the limitations of the resulting simple Reynolds number corrections. Simple corrections for the drag and lift coefficients are described in the following paragraphs. The procedures required to implement these corrections in a comprehensive rotorcraft analysis (specifically ref. 1) are given in the Appendix.

Drag Coefficient

In order to develop a method for correcting the drag coefficient data in an airfoil table, an explicit equation is required for the dependence on Reynolds number, i.e.

$$c_{d_{min}} = \text{constant} * f(Re)$$

Correcting $c_{d_{min}}$ directly is not desirable, because it would be necessary to search the airfoil table for $c_{d_{min}}$ (or include a separate array of $c_{d_{min}}$ values); moreover, it would still be necessary to correct the drag due to lift. Therefore, only corrections for the total drag c_d are considered. It is expected that the skin friction drag would scale in the same manner at all lifts; in fact, it is found that the total drag varies with Reynolds number very much like the minimum drag coefficient varies (certainly to the accuracy of the corrections being developed here). Hence it is assumed that the drag varies with Reynolds number according to the equation

$$c_d = \text{constant} * f(Re)$$

where f(Re) is the universal scaling equation being used, and the constant is evaluated from the airfoil table drag value. It follows that the airfoil table drag coefficient c_{d_t}, at Reynolds number Re_t, is corrected to the drag at Reynolds number Re by the equation

$$c_d = c_{d_t}/K$$

where $K = f(Re_t)/f(Re)$.

The results of the preceding sections provide several choices for the function f(Re). Equations 1-6 for flat-plate skin friction drag give, respectively:

$$f(Re) = Re^{-0.5} \qquad \text{(Eq. 1a)}$$

$$f(Re) = Re^{-0.2} \qquad \text{(Eq. 2a)}$$

$$f(Re) = \frac{0.455}{(\log Re)^{2.58}} - \frac{A}{Re} \qquad \text{(Eq. 3a)}$$

$$f(Re) = (3.46 \log Re - 5.6)^{-2} \qquad \text{(Eq. 5a)}$$

$$f(Re) = (\log Re - 0.407)^{-2.64} \qquad \text{(Eq. 6a)}$$

Equation 4 is an implicit relation, which is not useful here. Equation 1a is for laminar boundary layers, while all the other equations are for turbulent boundary layers (eq. 3a includes the transition region for nonzero A). The similarity between the form of the skin friction drag curve (fig. 1) and the curves for airfoil minimum drag implies that these equations will be useful for airfoils as well.

The airfoil minimum drag coefficient plots (figs. 2-7) often show a constant slope over a significant Reynolds number range implying the scaling equation

$$f(Re) = Re^{-n}$$

This form also covers the laminar and turbulent flat plate skin friction equations above, with n = 0.5 (eq. 1a) and n = 0.2 (eq. 2a), respectively. The turbulent flat plate boundary layer equation is the source of the one-fifth power scaling law frequently used for helicopter airfoil table corrections. The curves presented in figs. 2-7 suggest values of n = 0.125 to 0.2, depending on the airfoil and the Reynolds number range.

With the power law for the scaling equation f(Re), the correction factor is $K = (Re/Re_t)$. Note that if Re/Re_t is a constant (under the conditions described in the previous section), it follows that K is a constant for the entire table in this case.

Perhaps the easiest correction to implement is the addition of a constant drag increment to the entire table:

$$c_d = c_{d_t} + \Delta c_d$$

The drag increment can be evaluated using the equations and figures of this

report. This approach, however, does not scale the drag due to lift well. The constant multiplicative factor of the preceding paragraph is probably more appropriate.

Lift Coefficient

A correction for the lift coefficient is required that will modify the maximum lift while leaving the lift-curve slope unchanged. This may be accomplished by correcting the airfoil table values $c_{\ell_t}(\alpha_t)$ as follows:

$$c_\ell = K\, c_{\ell_t}(\alpha/K)$$

where here

$$K = \alpha_{max}/(\alpha_{max})_t = c_{\ell_{max}}/(c_{\ell_{max}})_t$$

(It is assumed here that $c_\ell(0) = 0$). To implement this equation, it is necessary to add to the airfoil table a list of $c_{\ell_{max}}$ values, for each Mach number in the table.

The maximum lift coefficient plots (figs. 8-16) provide guidance for selecting the equation that will define the scaling of $c_{\ell_{max}}$ with Reynolds number. Often the curves have a constant slope over a significant Reynolds number range, which implies the equation

$$K = c_{\ell_{max}}/(c_{\ell_{max}})_t = (Re/Re_t)^n$$

where the constant n is a small positive number, say 0.125 to 0.2.

CONCLUSIONS

The available literature on experimental two-dimensional airfoil characteristics were examined to establish the influences of Reynolds number that must be considered for helicopter rotor analyses. The discussion focussed

on the effects of Reynolds number on the minimum drag and maximum lift. For a substantial range of Reynolds number, the minimum drag coefficient of an airfoil varies with Reynolds number in a manner similar to the variation of flat plate skin friction drag, although the airfoil characteristics may not show a transition region (depending on the test conditions). The drag generally decreases with Reynolds number. The effect of Reynolds number on drag is greater for rough airfoils and for thick airfoils. The maximum lift coefficient generally increases with Reynolds number. The influence of Reynolds number on lift is greater for thick airfoils and less for rough airfoils. Mach number effects must also be included when discussing the influence of Reynolds number. Attention must be given to the manner in which the Mach number was varied with Reynolds number for a given test. Evidence suggests that Reynolds number effects on $c_{\ell_{max}}$ diminish as the Mach number increases.

From the trends observed in the airfoil data, simple methods to correct for Reynolds number effects in helicopter rotor analyses were derived. Finally, it should be noted that the discrepancies observed between data from various sources made correlation of the results difficult. Standardization of wind-tunnel tests on two-dimensional airfoil characteristics is necessary to eliminate inconsistencies. This problem not only degrades the accuracy of the airfoil characteristics used in rotor analyses, but also makes it more difficult to assess the influence of Reynolds number on these characteristics.

APPENDIX

Modifications to Comprehensive Rotorcraft Analysis Required To Implement The Simple Reynolds Number Corrections

This appendix presents the specific modifications to the equations in the Comprehensive Analytical Model of Rotorcraft Aerodynamics and Dynamics (ref. 1) that are required to implement the simple Reynolds number corrections described in this report.

Reynolds Number

In order to calculate the Reynolds number as required to implement the corrections, the air viscosity must be included in the environment model (pp. 127-128, ref. 1). The viscosity is obtained from the equation:

$$\mu = \mu_0 \frac{(T/T_0)^{3/2}}{0.723\,(T/T_0) + 0.277}$$

where T/T_0 is the ratio of the temperature to the sea level standard temperature T_0, and the sea level standard viscosity has the value

$$\mu_0 = 3.7373\text{ E-7 lb-sec/ft}^2 = 1.7894\text{ E-5 N-sec/m}^2$$

For yawed flow, the Reynolds number will be greater than for unyawed flow: $V_{yaw} = V/\cos\lambda$ and $c_{yaw} = c/\cos\lambda$ (where λ is the yaw angle), so $Re_{yaw} = V_{yaw}\, c_{yaw}/\nu = Re/\cos^2\lambda$.

Drag Coefficient

The drag coefficient (p. 120, ref. 1) is evaluated with the following equation, incorporating effects of yawed flow, dynamic stall, and now the Reynolds number correction:

$$c_d = \frac{1}{K\cos\lambda}\, c_{d_t}(\alpha_d \cos\lambda) + \Delta c_{d_{DS}}$$

or

$$c_d = \frac{1}{\cos\lambda} c_{d_t}(\alpha_d \cos\lambda) + \Delta c_{d_{Rey}} + \Delta c_{d_{DS}}$$

where λ is the yaw angle, α_d is a delayed angle of attack accounting for dynamic stall effects, and $\Delta c_{d_{DS}}$ is a drag increment due to dynamic stall. The Reynolds number correction factor is $K = f(Re_t)/f(Re)$, where the function f can be chosen from eqs. 1a to 6a. Alternatively, a single drag increment $\Delta c_{d_{Rey}}$ can be used

Lift Coefficient

The lift coefficient (pp. 119-120, ref. 1) is evaluated with the following equation, incorporating effects of yawed flow, dynamic stall, and now the Reynolds number correction:

$$c_\ell = \frac{K}{\cos^2\lambda}\left(\frac{\alpha}{\alpha_d}\right)\left[c_{\ell_t}\left(\frac{\alpha_d \cos^2\lambda}{K}\right) - c_{\ell_t}(o)\right] + c_{\ell_t}(o) + \Delta c_{\ell_{DS}}$$

where $c_{\ell_t}(o)$ is the lift coefficient at zero angle of attack, λ is the yaw angle, α_d is a delayed angle of attack accounting for dynamic stall effects, and $\Delta c_{\ell_{DS}}$ is a lift increment due to dynamic stall. The Reynolds number correction factor is $K = (Re/Re_t)^n$.

Airfoil Table

The airfoil table (pp. 112-115, ref. 1) must be modified to include the following additional data required to implement the Reynolds number corrections: Reynolds number Re, maximum lift coefficient $c_{\ell_{max}}$, perhaps minimum drag coefficient $c_{d_{min}}$, and perhaps angle of zero lift α_{ZL} (all as a function of Mach number).

REFERENCES

1. Johnson, W.: A Comprehensive Analytical Model of Rotorcraft Aerodynamics and Dynamics. NASA TM 81182, June 1980.

2. Schlichting, H.: Boundary Layer Theory. New York, McGraw Hill Book Company, 1960.

3. Hoerner, S.F.: Fluid-Dynamic Drag. New Jersey, Published by the Author, 1965.

4. Abbott, I., von Doenhoff, A.: Theory of Wing Sections. New York, Dover Publications, Inc., 1959.

5. Jacobs, E., Sherman, A.: Airfoil Characteristics as Affected by Variations of the Reynolds Number. NACA Rept. 586, 1936.

6. Jacobs, E., Abbott, I.: Airfoil Section Data Obtained in the N.A.C.A. Variable Density Tunnel as Affected by Support Interference and Other Corrections. NACA Rept. 669, 1939.

7. Jacobs, E., Clay, W.: Characteristics of the N.A.C.A. 23012 Airfoil from Tests in the Full-Scale and Variable-Density Tunnels. NACA Rept. 530, 1935.

8. Goett, H., Bullivant, W.: Tests of N.A.C.A. 0009, 0012, and 0018 Airfoils in the Full-Scale Tunnel. NACA Rept. 647, 1938.

9. Loftin, L., Smith, H.: Aerodynamic Characteristics of 15 NACA Airfoil Sections at Seven Reynolds Numbers From 0.7×10^6 to 9.0×10^6. NACA TN 1945, 1949.

10. Schaefer, R., Loftin, L., Horton, E.: Two-Dimensional Investigation of Five Related NACA Airfoil Sections Designed for Rotating Wing Aircraft. NACA TN 1922, 1949.

11. Loftin, L., Poteat, M.: Aerodynamic Characteristics of Several NACA Airfoil Sections at Seven Reynolds Numbers from 0.7×10^6 to 9.0×10^6. NACA RM L8B02, 1948.

12. von Doenhoff, A., Nuber, R.: Drag Measurements at High Reynolds Numbers of a 100-Inch-Chord NACA 23016 Practical Construction Wing Section Submitted by Chance Vought Aircraft Company. NACA War Rept. L-752 (MR June 1944), 1944.

13. Loftin, L., Bursnall, W.: The Effects of Variations in Reynolds Number Between 3.0×10^6 and 25.0×10^6 Upon the Aerodynamic Characteristics of a Number of NACA 6-Series Airfoil Sections. NACA TN 1773, 1948.

14. Racisz, S.: Effects of Independent Variations of Mach Number and Reynolds Number on the Maximum Lift Coefficients of Four NACA 6-Series Airfoil Sections. NACA TN 2824, 1952.

15. Noonan, K., Bingham, G.: Aerodynamic Characteristics of Three Helicopter Rotor Airfoil Sections at Reynolds Numbers From Model Scale to Full Scale at Mach Numbers From 0.35 to 0.90. NASA TP 1701, 1980.

16. McCullough, G.: The Effect of Reynolds Number on the Stalling Characteristics and Pressure Distributions of Four Moderately Thin Airfoil Sections. NACA TN 3524, 1955.

17. Gregory, N., O'Reilly, C.: Low-Speed Aerodynamic Characteristics of NACA 0012 Aerofoil Section, including the Effects of Upper-Surface Roughness Simulating Hoar Frost. A.R.C. 31 719, 1970.

18. Becker, J.: Boundary-Layer Transition on the NACA 0012 and 23012 Airfoils in the 8-Foot High-Speed Wind Tunnel. NACA War Rept. L-682 (ACR January 1940), 1940.

19. Muse, T.: Some Effects of Reynolds and Mach Numbers on the Lift of an NACA 0012 Rectangular Wing in the NACA 19-Foot Pressure Tunnel. NACA War Rept. L-406 (CB 3E29), 1943.

20. Spreiter, J., Steffen, P.: Effect of Mach and Reynolds Numbers on Maximum Lift Coefficient. NACA TN 1044, 1946.

21. van den Berg, B.: Reynolds Number and Mach Number Effects on the Maximum Lift and the Stalling Characteristics of Wings at Low Spees. NLR TR 69025U, 1969.

22. Fitzpatrick, J., Schneider, W.: Effects of Mach Number Variation Between 0.07 and .34 and Reynolds Number Variation Between 0.97×10^6 and 8.10×10^6 on the Maximum Lift Coefficient of a Wing of NACA 64-210 Airfoil Sections. NACA TN 2753, 1952.

23. Furlong, G., Fitzpatrick, J.: Effects of Mach Number and Reynolds Number on the Maximum Lift Coefficient of a Wing of NACA 230-Series Airfoil Sections. NACA TN 1299, 1947.

TABLE 1: TEST CONDITIONS

SOURCE	REF	WIND TUNNEL	CHORD	SPAN	MACH NUMBER OR SPEED RANGE	PRESSURE RANGE	AIRFOILS
NACA REPT. 586	5	VDT	.127m	.762m	$M \cong .06$ *	.25-.20 atm	0009, 0012, 0015 0018, 2412, 4412 6412, 23012
NACA REPT. 669	6	VDT	.127m	.762m		.25-.20 atm	0012 aspect ratio 6 wing
NACA REPT. 530	7	VDT FST	.127m 1.8288m	.762m 10.9728m	13.41-33.53 m/sec	1 atm	23012 aspect ratio 6 wing
NACA REPT. 647	8	FST	1.8288m	10.9728m	$.04 \leq M \leq .11$*	1 atm	0009,0012 aspect ratio 6 wing
NACA TN 1945	9	LTT	.6096m	2-D	$M \leq .15$	1 atm	0012, 23012
NACA TN 1922	10	LTT	.6096m	2-D			11-H-09, 12-H-12, 13-H-12, 14-H-12, 15-H-15
NACA RM L8B02	11	LTT	.6096m	2-D	$M \leq .15$	1 atm	23012, 23015
Abbot and von Doenhoff	4	TDT	.6096m	2-D	$M \leq .17$		23012

*as stated in reference 20

TABLE 1: CONTINUED

SOURCE	REF	WIND TUNNEL	CHORD	SPAN	MACH NUMBER OR SPEED RANGE	PRESSURE RANGE	AIRFOILS
NACA WAR REPT. L-752	12	TDT	2.54m	2-D			23016
NACA TN 1773	13	TDT	.6096m	2-D	low		63-006, 63-009 63_1-012, 63_3- 018 64-006, 65-006
NACA TN 2824	14	TDT	.6096m	2-D	$M \cong .3$		65-006
NASA TP 1701	15	Langley[1] Transonic Tunnel	.0787m	2-D	$M \cong .4$	1.19-6.12 atm	SC1095, SC1095-R8 0012 C-deg tab
NACA TN 3524	16	Ames[2] Wind Tunnel	1.524m 1.3716m	2-D	$.03 \leq M \leq .17$ $.05 \leq M \leq .22$		0007, 0008 0006
A.R.C. 31 719	17	NPL[3] Low Speed Wind Tun.	.762m	2-D	$M \leq .16$		0012
NACA WAR REPT. L-682	18	NACA[4] High Speed Wind Tun.	.6096m 1.524m	2-D	$.29 \leq M \leq .59$ $.11 \leq M \leq .20$		0012

1 0.1524 - by 0.7112- meter
2 2.1336- by 3.048- meter
3 3.9624- by 2.7432- meter
4 2.4384 meter

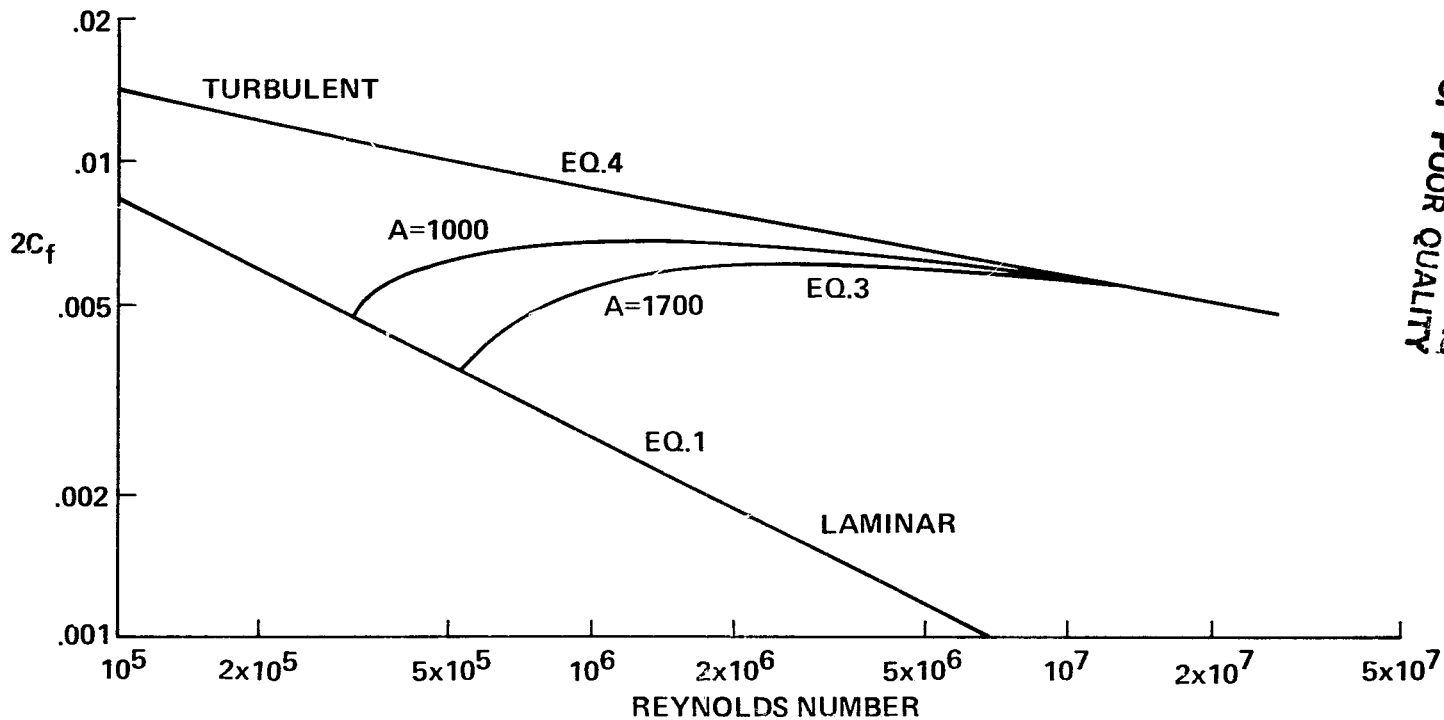

Figure 1. Skin friction coefficient of a flat plate at zero incidence

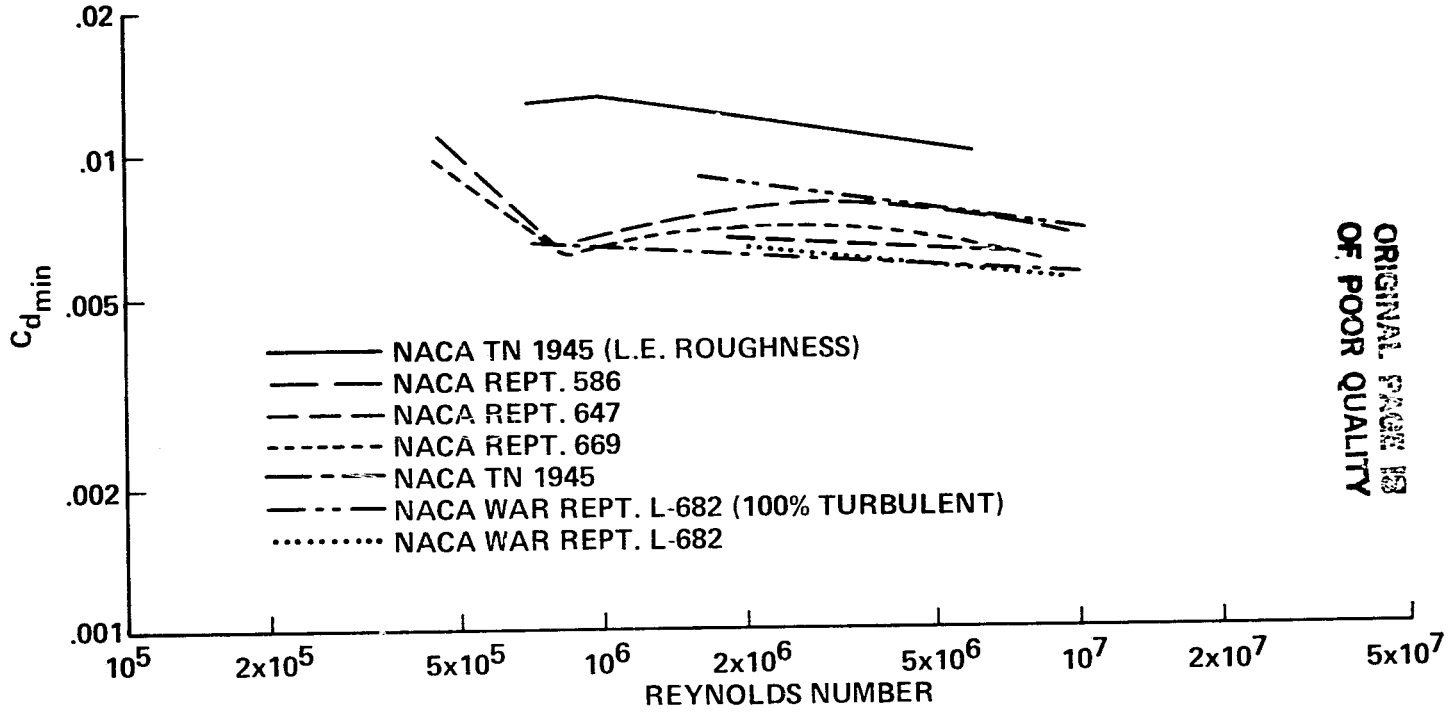

Figure 2. Minimum drag coefficient for NACA 0012 airfoil

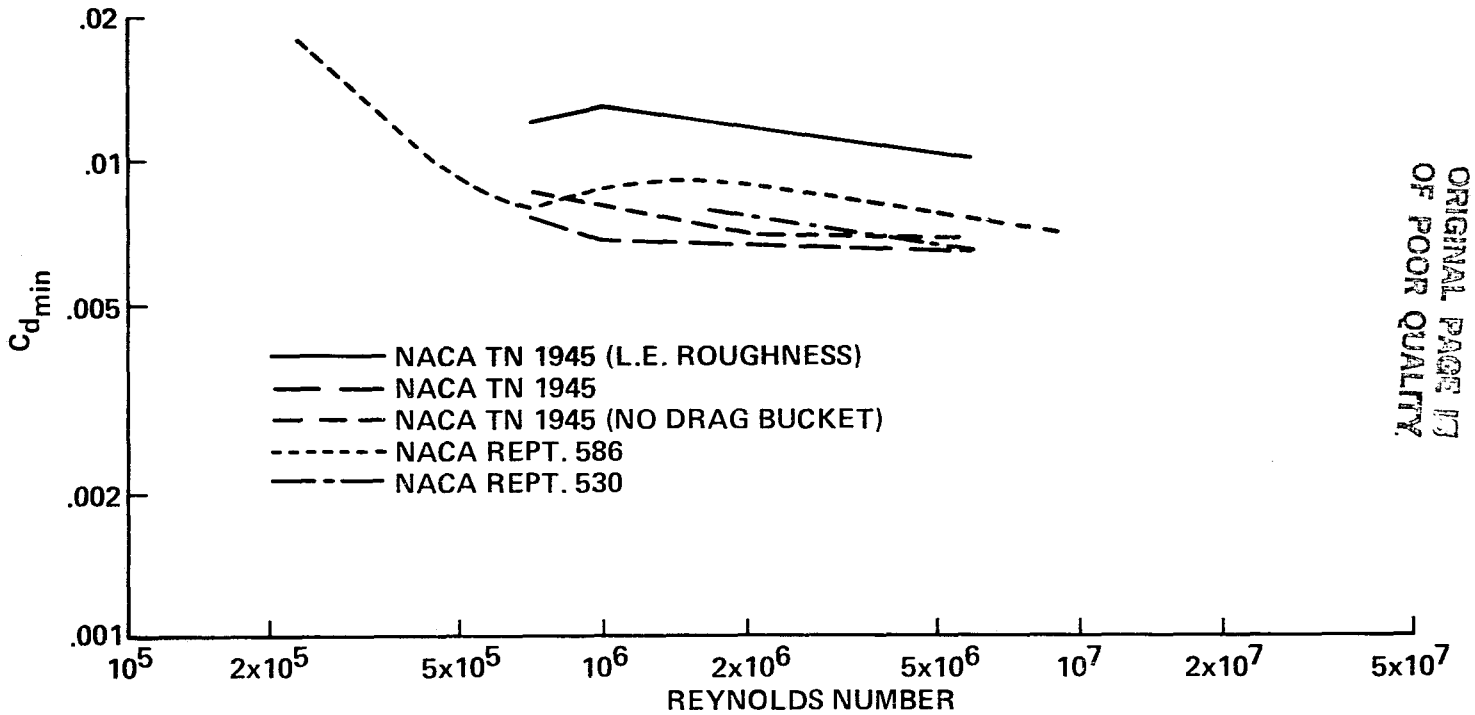

Figure 3. Minimum drag coefficient for NACA 23012 airfoil

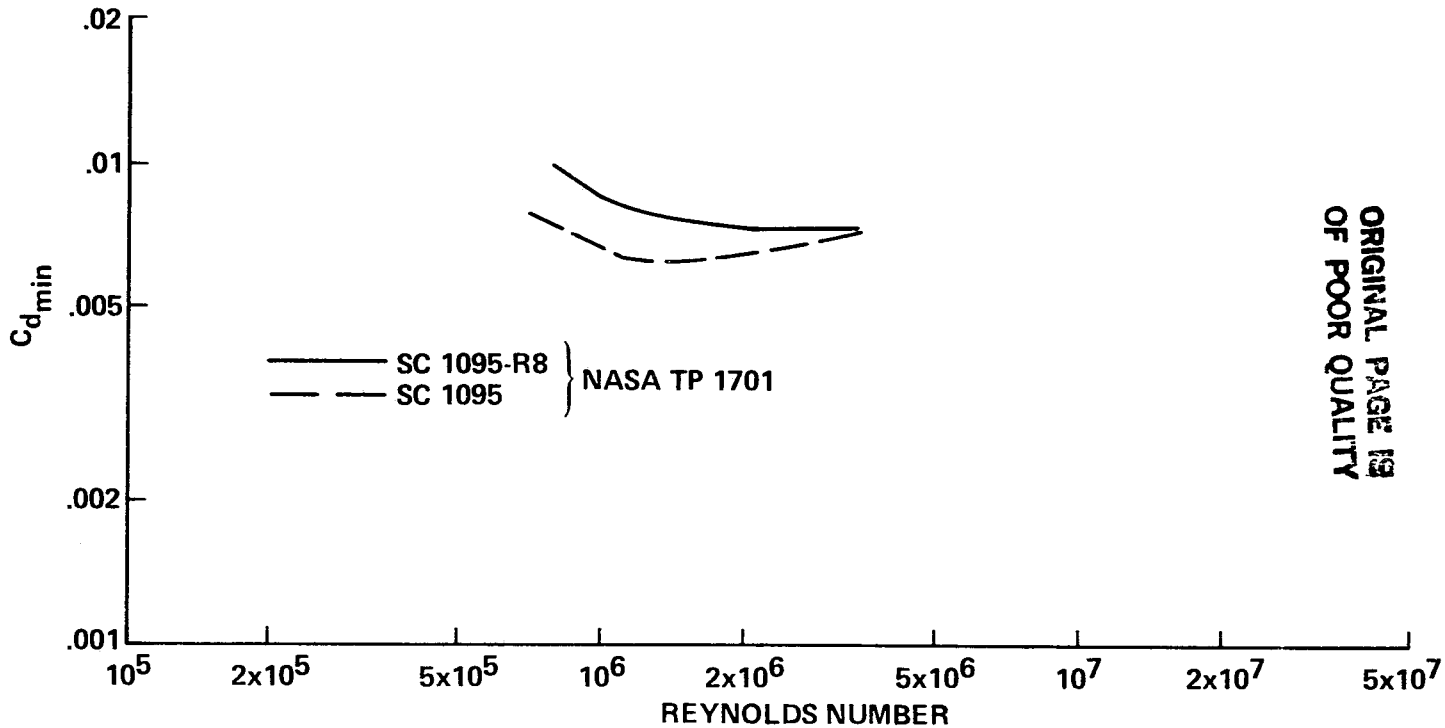

Figure 4. Minimum drag coefficient for SC1095 and SC1095-R8 airfoils

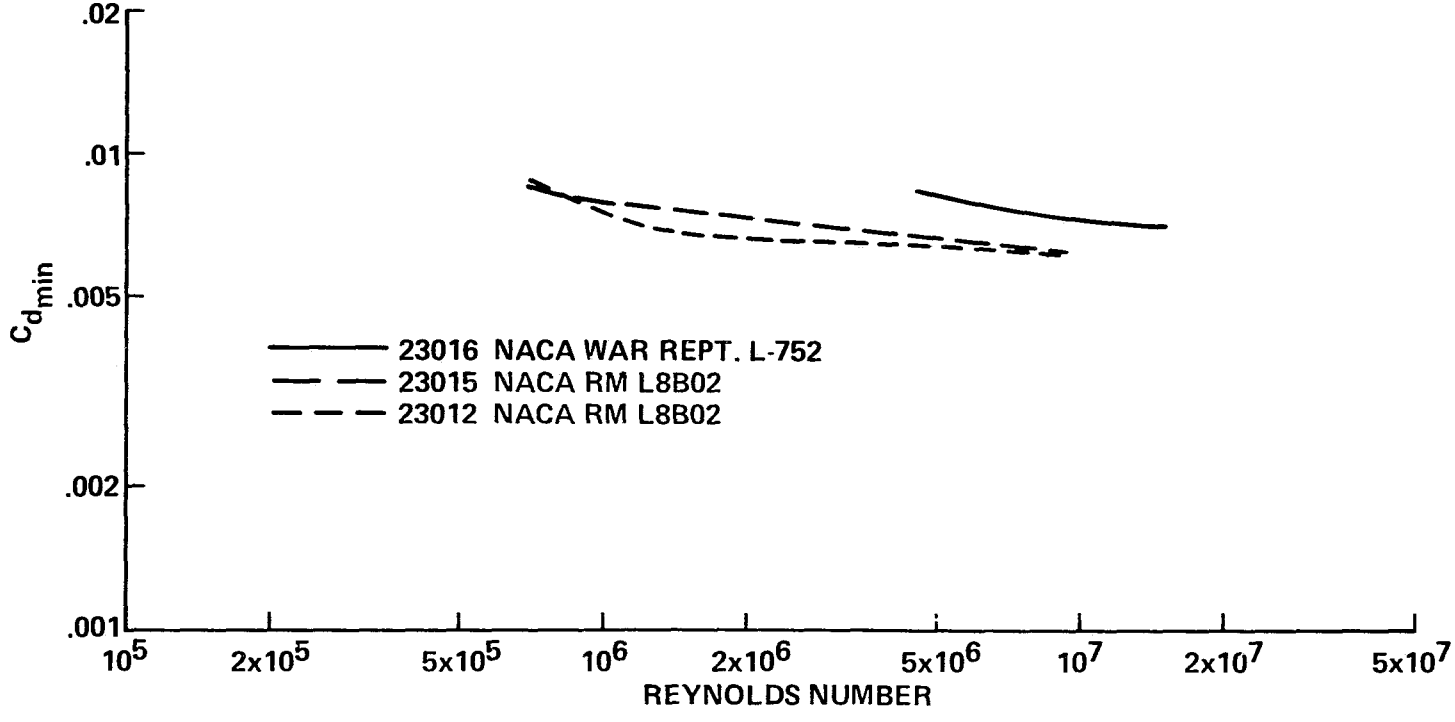

Figure 5. Minimum drag coefficient for NACA 230-series airfoils: effect of thickness

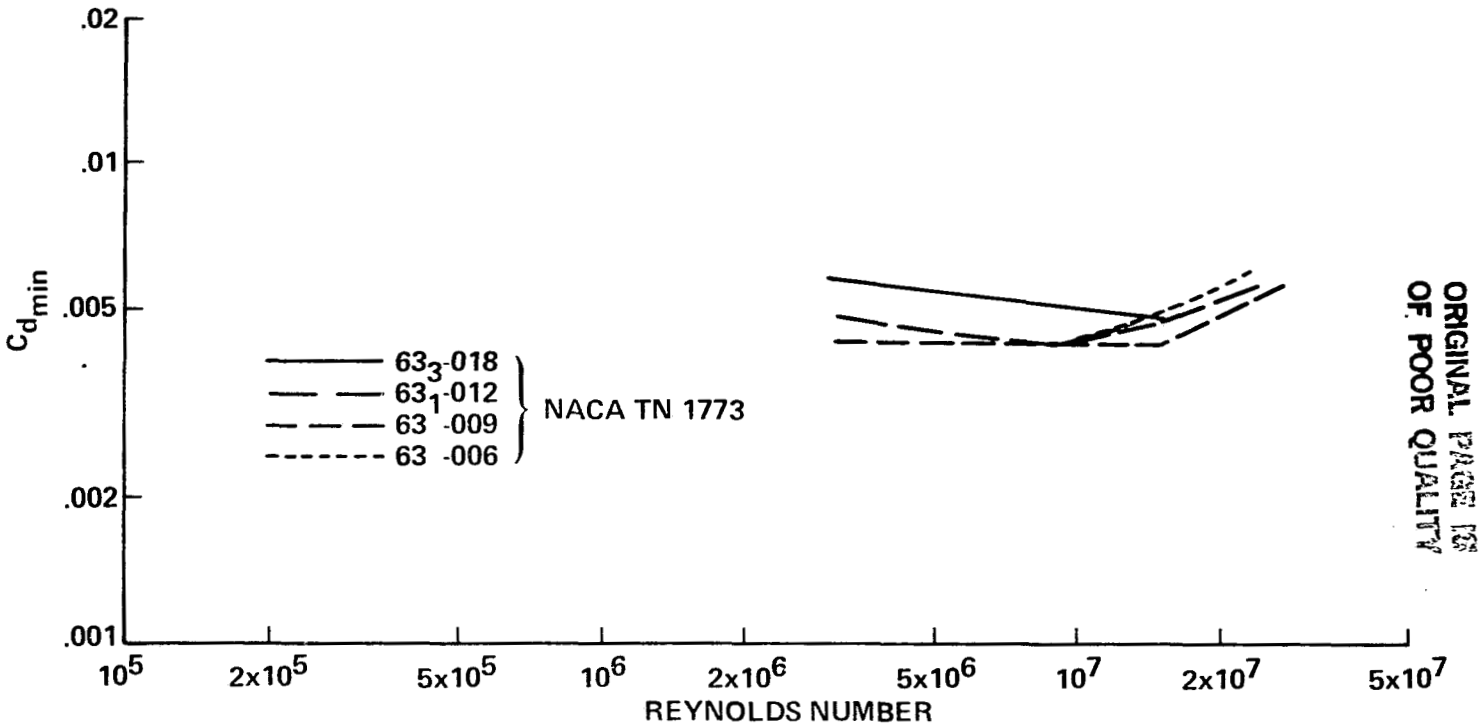

Figure 6. Minimum drag coefficient for NACA 63-series airfoils: effect of thickness

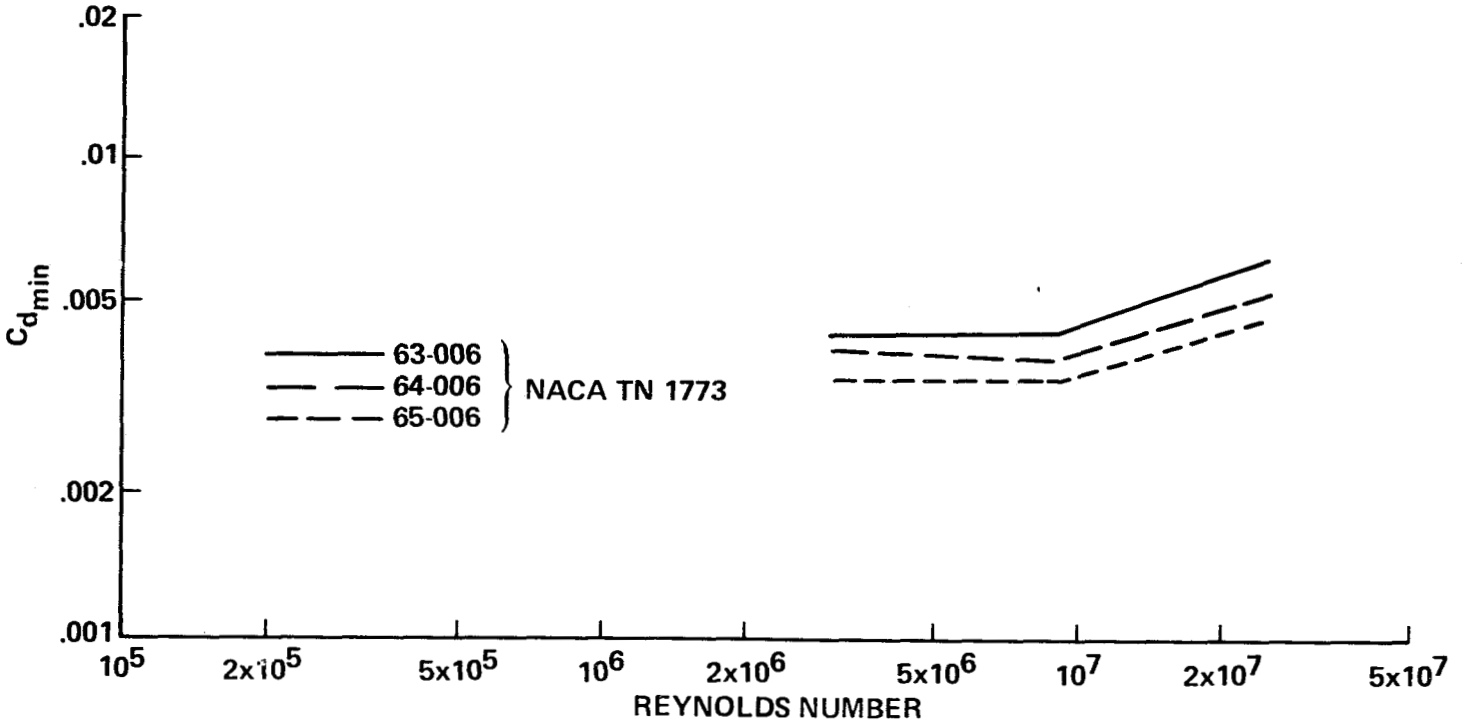

Figure 7. Minimum drag coefficient for NACA 6-series airfoils: effect of thickness form

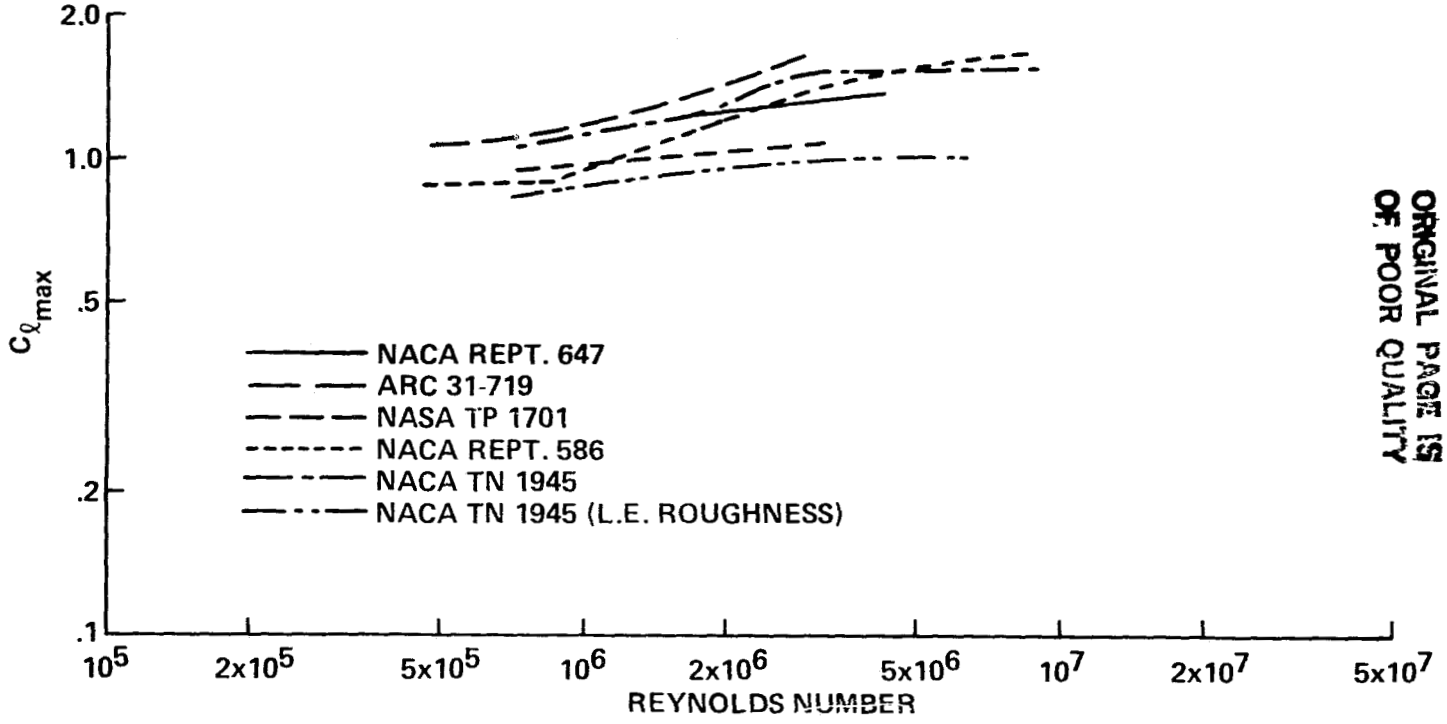

Figure 8. Maximum lift coefficient for NACA 0012 airfoil

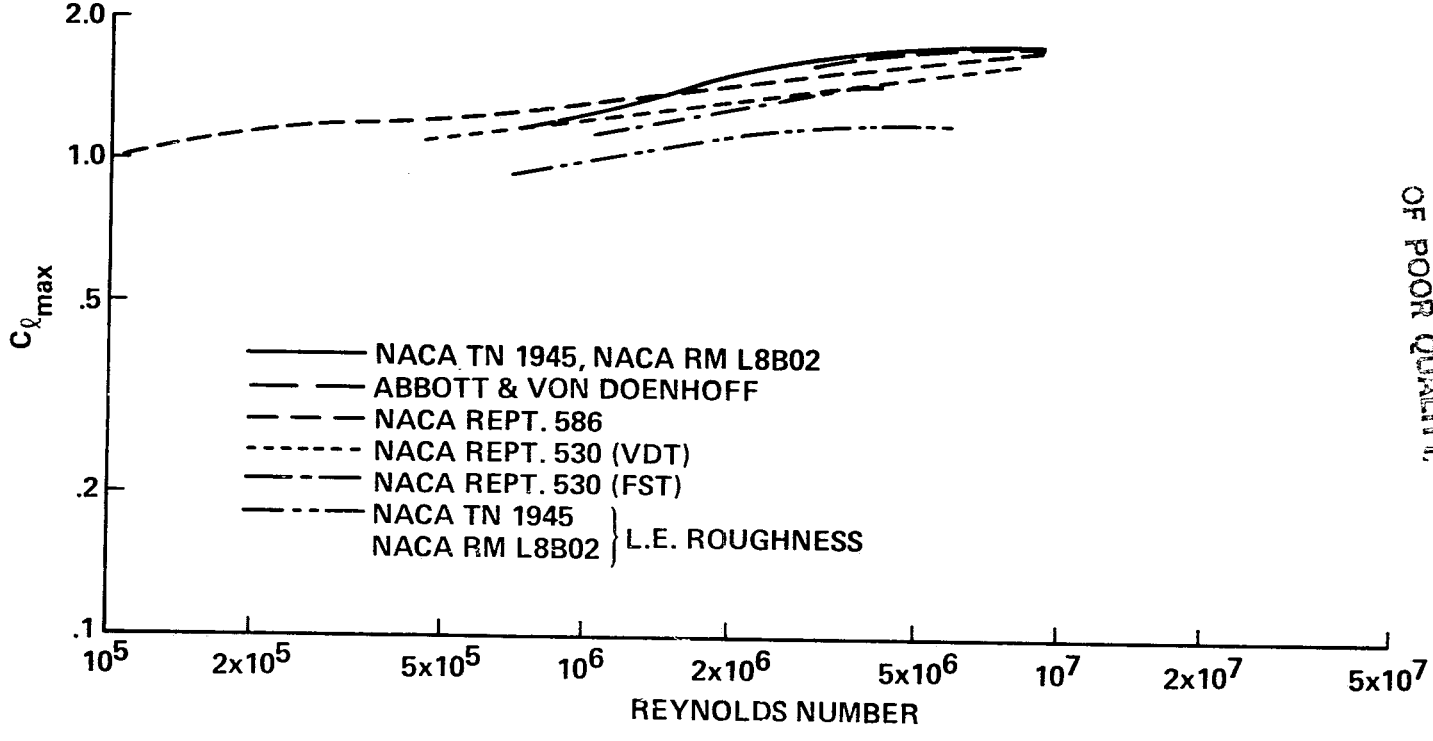

Figure 9. Maximum lift coefficient for NACA 23012 airfoil

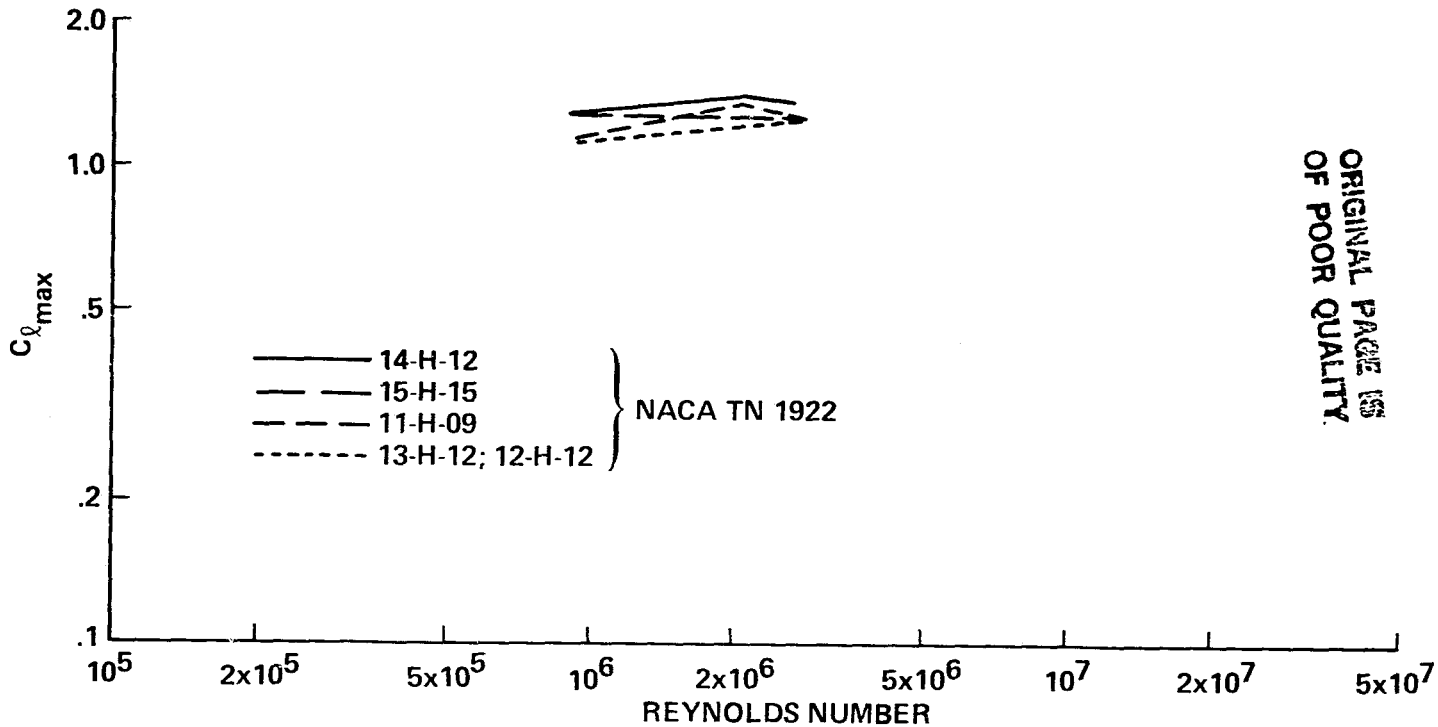

Figure 10. Maximum lift coefficient for airfoils designed for rotor blades

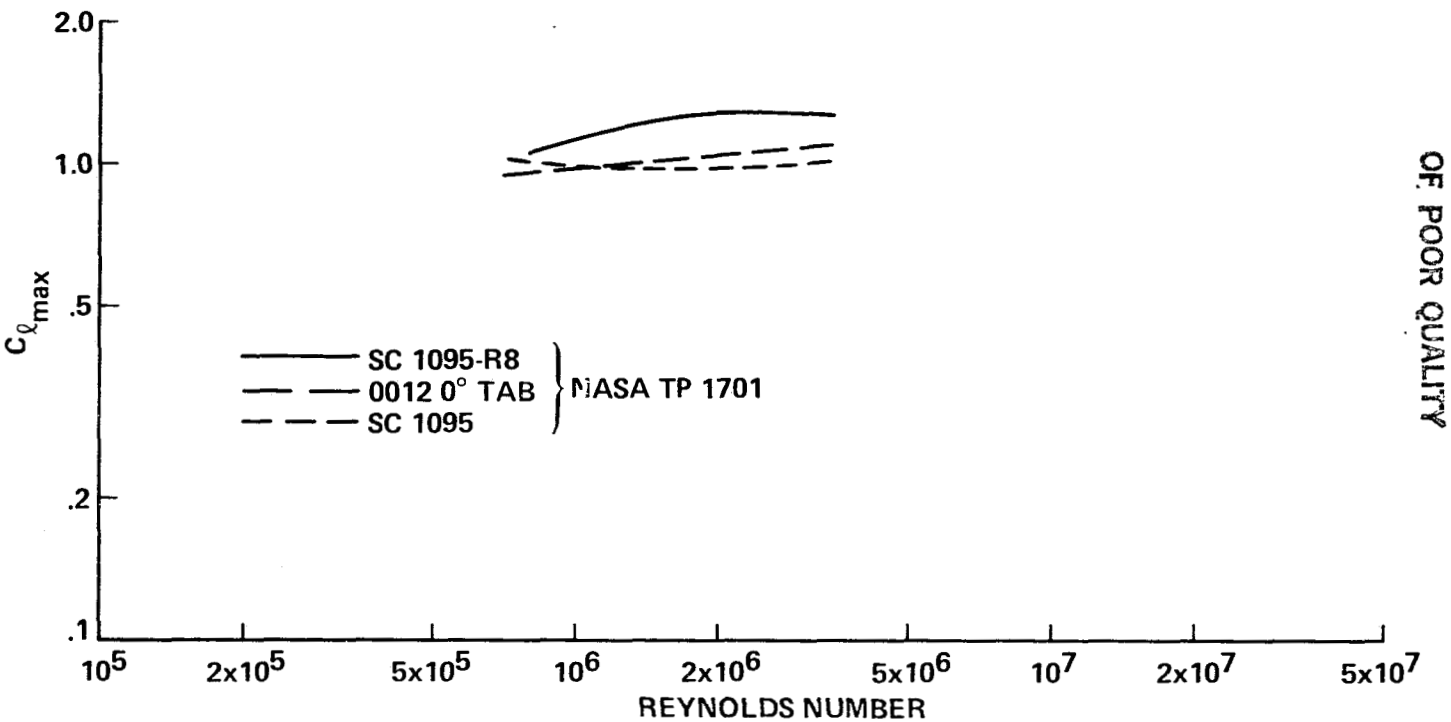

Figure 11. Maximum lift coefficient for SC1095, SC1095-R8, and 0012 (0 deg tab) airfoils

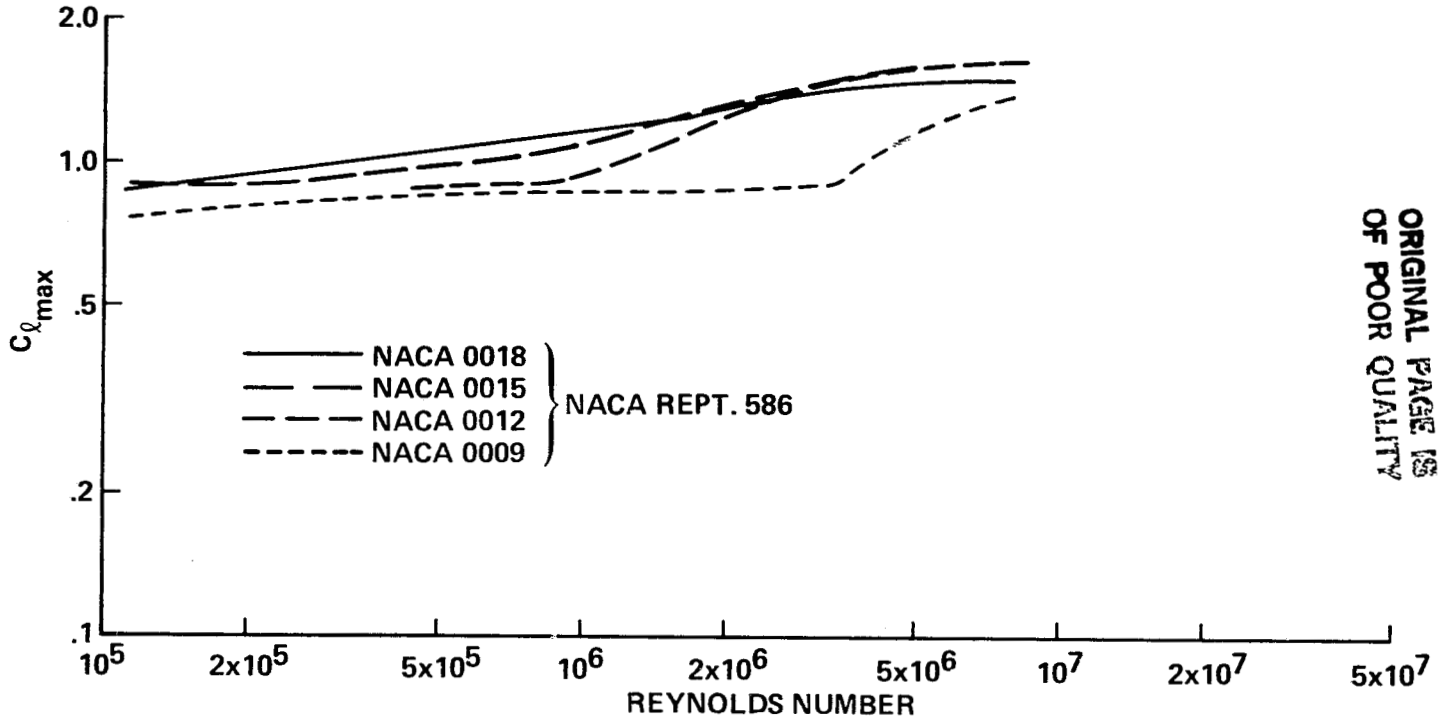

Figure 12. Maximum lift coefficient for NACA symmetrical airfoils: effect of thickness

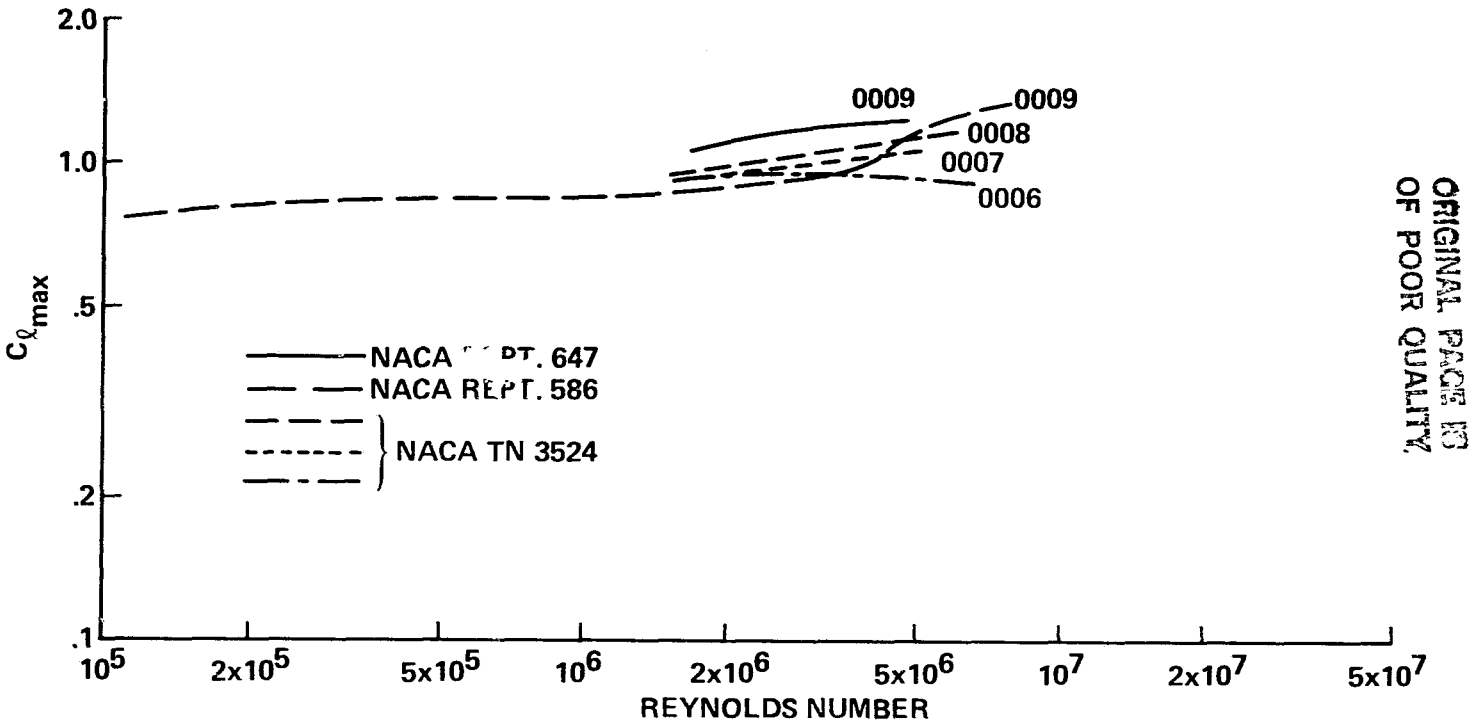

Figure 13. Maximum lift coefficient for NACA symmetrical airfoils: effect of thickness

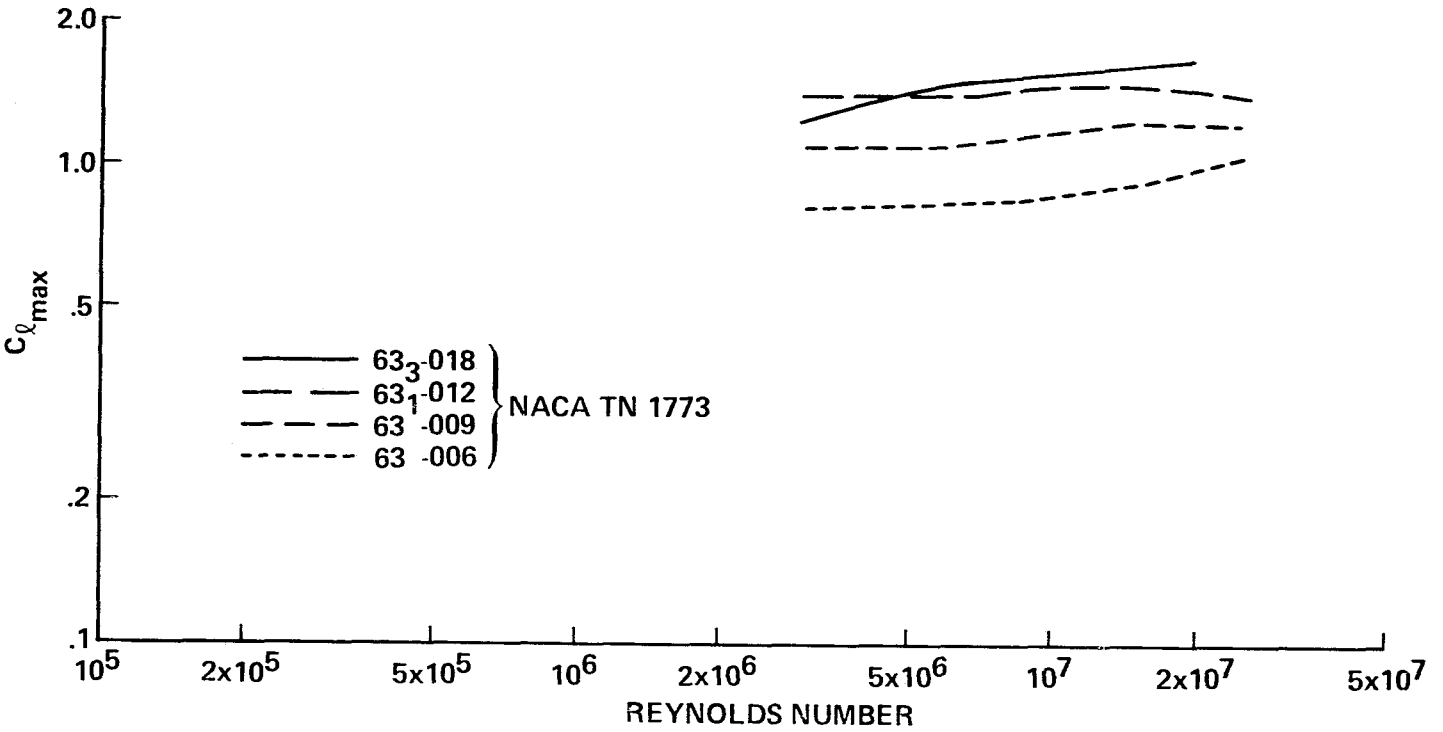

Figure 14. Maximum lift coefficient for NACA 63-series airfoils: effect of thickness

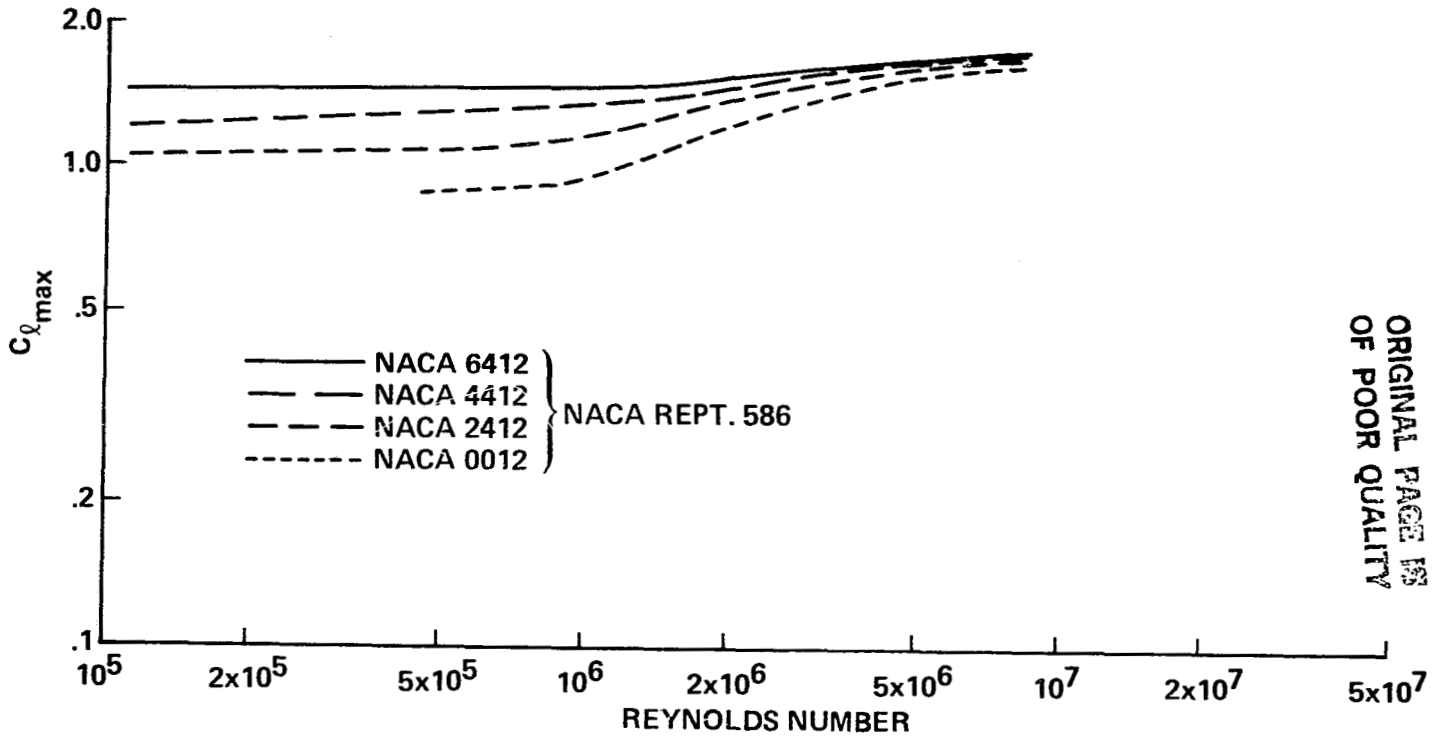

Figure 15. Maximum lift coefficient for NACA 4-digit series airfoils: effect camber

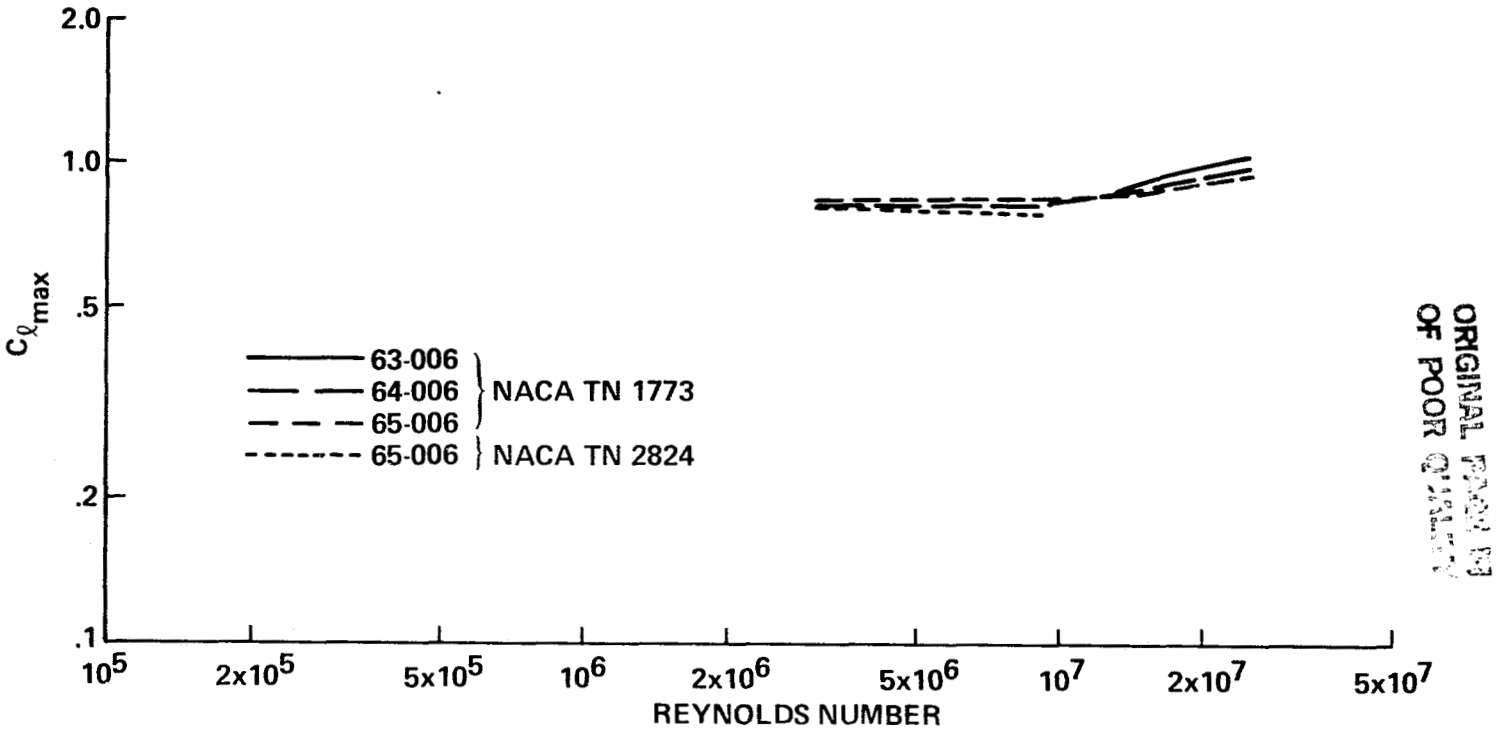

Figure 16. Maximum lift coefficient for NACA 6-series airfoils: effect of thickness form